IEEE Access
Multidisciplinary | Rapid Review | Open Access Journal

Received August 8, 2020, accepted August 19, 2020, date of publication August 24, 2020, date of current version September 9, 2020.

Digital Object Identifier 10.1109/ACCESS.2020.3018792

Threshold Based Signal Detection and the Average Symbol Error Probability for Downlink NOMA Systems With *M*-ary QAM

HONGJUN XU, (Member, IEEE), AND NARUSHAN PILLAY
School of Engineering, University of KwaZulu-Natal, Durban 4041, South Africa
Corresponding author: Narushan Pillay (pillayn@ukzn.ac.za)

ABSTRACT Non-orthogonal multiple access (NOMA) is a technique which allows multiple users to share the same radio access resources. However, there exist interferences among these users in the NOMA system. These interferences need to be taken into account in the signal detection and error performance analysis. In the downlink NOMA system, the far user detects its signal by treating the near user's signal as interference, while the near user employs successive interference cancellation (SIC) to detect its signal. Based on the conventional signal detection, it is not straightforward to derive the error performance for both the far user and near user. By analyzing the constellation relationships between the far user's signal and superposition coded (SC) signal, and the near user's signal and SC signal, in this article, a simple threshold based detection algorithm is proposed to detect both the far user's signal and near user's signal. Furthermore, by aid of the constellation relationships, in this article, simple expressions of the average symbol error probability (ASEP) with squared *M*-ary quadrature amplitude modulation for both the far user and near user are easily derived in Rayleigh fading channels. Simulation results validate the derived theoretical ASEP results.

INDEX TERMS Downlink non-orthogonal multiple access, maximum likelihood detection, threshold based detection, signal constellation, successive interference cancellation, superposition coded signals, symbol error probability.

I. INTRODUCTION

Nowadays there is an ever-growing demand for high data transmission rates and reliability in wireless communication systems. Traditionally, multiplexing is a technique to improve data transmission rate. Multiple-input multiple-output (MIMO) is a technique to provide multiplexing gain in wireless communications. Recently non-orthogonal multiple access (NOMA) has been considered as a promising technique to improve data transmission rate in 5G wireless communication system [1], [2]. In the NOMA system, all users share the same radio access resources, thus allowing a further improvement in spectral efficiency. In the conventional NOMA system, superposition coding is employed at the transmitter in order to enable sharing of the common resources for different users, and successive interference cancellation (SIC) is used to detect the superposition coded (SC) signals at the receiver [2], [3].

There are two kinds of NOMA systems, uplink NOMA (UL-NOMA) and downlink NOMA (DL-NOMA) systems. The research problems in NOMA systems can be mainly categorized into error performance analysis [4]–[8], outage probability analysis [9], [10], power allocation [11] and system capacity or ergodic sum-rate [12], [13]. In this article, we mainly focus on error performance analysis of the DL-NOMA systems. In general, the DL-NOMA system contains one base station (BS) and two users, a far user and a near user. Due to the non-orthogonal multiple user access there is an interference at the receiver for either the far user or the near user. Most of the work in the literature has taken into account the interference to detect the users' signal and to analyze the error performance. In the literature, the conventional signal detection is that the far user detects its signal by regarding the near user's signal as interference, and the near user uses SIC to detect its signal. In [4] and [7], the error performance of the DL-NOMA system is analyzed based on the conventional signal detection. The derivation of the error performance is also based on two dimensional signal constellations and the procedure to derive the error performance is not concise. Since an *M*-ary quadrature amplitude modulation (*M*QAM) symbol is composed of independent in-phase and quadrature components, [5] firstly analyzed error performance based

The associate editor coordinating the review of this manuscript and approving it for publication was Md. Arafatur Rahman.

on only the one dimensional in-phase or pulse amplitude modulation (PAM) signal. The derivation of error probability for the far user is based on the relationship between the SC signal and the far user's signal and is not straightforward. However, the derivation of error performance for the near user is too long because by examining and comparing the decision regions and distant parameters, [5] classifies all signals into three types. Then, by considering the relationship between PAM and QAM, [5] derived error performance expressions for MQAM. However, these expressions are only derived for additive white Gaussian noise (AWGN) channels and not fading channels. Meanwhile, the work of [6] also analyzed the error performance based on interference cancellation. Since the probability density function (PDF) of the summation of interference and noise is not Gaussian distributed, the error performance expression is not simple. Finally, taking into account interference, [8] derived the error performance based on one dimensional signals. The average symbol error probabilities (ASEPs) for both the far user and near user are derived in Rayleigh fading channels considering imperfect SIC. However, the derived error performance expressions are too complicated.

In summary, most of the above work considered interferences to derive error performance but the derivations are not concise. In this article, we will not take into account the interference to derive the error performance. Instead, by analyzing the constellations of the individual user's signal and the SC signal, we firstly propose a threshold based simple signal detection algorithm for both the far user and near user. Then aided by the proposed detection algorithm, we easily derive the ASEPs for both the far user and near user.

Hence, the main contributions of this article are summarized as:

1) A threshold based simple signal detection for both the far user and near user is proposed. The proposed threshold based detection has low detection complexity compared to the conventional detection.
2) An approach to derive error performance for the individual user is proposed. The approach is to convert the derivation of error performance for the individual user's symbols into the error performance of the SC symbols.

The remainder of the paper is organized as follows: In Section II, the system model is presented. The constellation analysis of the individual users' symbol and the SC symbols is presented in Section III. The conventional detection scheme and the proposed threshold based detection algorithm are presented in Section IV. The ASEPs for both far user and near user are derived in Section V. In Section VI, the numerical results are demonstrated. Finally, the paper is concluded in Section VII.

Notation: Bold lowercase and uppercase letters are used for vectors and matrices, respectively. $[\cdot]^T$, $(\cdot)^H$, $|\cdot|$ and $\|\cdot\|_F$ represent the transpose, Hermitian, Euclidean and Frobenius norm operations, respectively. $E\{\cdot\}$ is the expectation operation. $j = \sqrt{-1}$ is a complex number. A complex symbol x has the real or in-phase part x^I and imaginary or quadrature part x^Q, such that $x = x^I + jx^Q$.

II. SYSTEM MODEL

The conventional DL-NOMA system has been documented in the literature [4]. The conventional DL-NOMA system consists of one BS and two users which are denoted as User n and User f. User n is an intra-cell user or near user, while User f is a cell-edge user or far user. Relatively, User n experiences good channel conditions, while User f experiences severe channel conditions. In the DL-NOMA system, the BS communicates with User n and User f on the same radio access resources, frequency and time through superposition coding. Let Ω_u be the signal set of the squared QAM with modulation order M_u, $u \in [n, f]$, x_n and x_f be the modulated symbols to be transmitted to Users n and f, $x_n \in \Omega_n$ and $x_f \in \Omega_f$. Similar to the discussion in [4], in this article, we will consider $M_f \leq M_n$ because User f experiences severe channel conditions. In the system model, it is also assumed that $E\{|x_n|^2\} = E\{|x_f|^2\} = \varepsilon$. By multiplying x_n and x_f with different power coefficients and summing them, the SC signal x_{sc} is given by:

$$x_{sc} = \sqrt{\alpha_n} x_n + \sqrt{\alpha_f} x_f, \tag{1}$$

where $\alpha_f = 1 - \alpha_n$. Since $E\{|x_n|^2\} = E\{|x_f|^2\} = \varepsilon$, it follows that $E\{|x_{sc}|^2\} = \varepsilon$.

In the conventional DL-NOMA system, it is also assumed that both User n and User f have a single receive antenna [4]. However, in this article, we extend the single receive antenna into N_r receive antennas at the receivers of User n and User f. The received signal at User u is given by:

$$\boldsymbol{y}_u = \boldsymbol{h}_u x_{sc} + \boldsymbol{w}_u, \tag{2}$$

where $\boldsymbol{y}_u \in \mathbb{C}^{N_r \times 1}$ is the signal vector received at the receiver of User u. $\boldsymbol{h}_u \in \mathbb{C}^{N_r \times 1}$ is the channel coefficient vector between the BS and User u. $\boldsymbol{w}_u \in \mathbb{C}^{N_r \times 1}$ is the AWGN vector. The entries of both $\boldsymbol{h}_u$ and $\boldsymbol{w}_u$ are mutually independent and identically distributed (i.i.d.) complex Gaussian random variables (RVs) distributed as $CN(0, \sigma_u^2)$ and $CN(0, \frac{\varepsilon}{\rho})$, where ρ is the signal-to-noise ratio (SNR) at each receive antenna.

It is also assumed that $\sigma_n^2 > \sigma_f^2$ because User n experiences good channel conditions, while User f experiences severe channel conditions. It is further emphasized that the key idea in the DL-NOMA system is to allocate more power to the user with severe channel conditions [5]. Thus $\alpha_f > \alpha_n$ is held in (1).

III. CONSTELLATION ANALYSIS OF THE SC SYMBOLS

The constellation of the SC symbols is essentially important to signal detection and error performance analysis. In the DL-NOMA system, the individual User u only receives $\boldsymbol{h}_u x_{sc} + \boldsymbol{w}_u$, not their own signal $\boldsymbol{h}_u x_u + \boldsymbol{w}_u$. The User u needs to detect or extract x_u from $\boldsymbol{h}_u x_{sc} + \boldsymbol{w}_u$. That motivates us to analyze the signal relationship between x_{sc} and x_u. In this section, we focus on constellation analysis of the SC symbols. Since QAM is composed of independent in-phase and

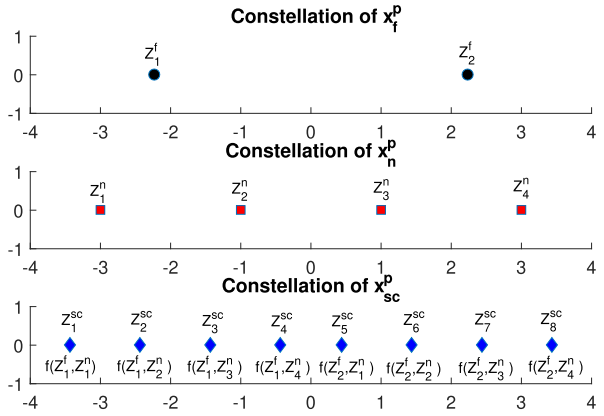

FIGURE 1. The constellations of x_f^p, x_n^p and x_{sc}^p with $\alpha_f = 0.75$ and $\alpha_n = 0.25$.

quadrature components, the constellation of the SC symbols is also composed of independent in-phase and quadrature component constellations. In this section, we only analyze a one dimensional constellation of the SC symbol, either in-phase or quadrature component.

Let $x_{sc} = x_{sc}^I + jx_{sc}^Q$, $x_n = x_n^I + jx_n^Q$ and $x_f = x_f^I + jx_f^Q$ in (1), where $x_u^p \in \Omega_u^p$, $p \in [I, Q]$ and Ω_u^p is the signal set of PAM with modulation order $K_u = \sqrt{M_u}$. $x_{sc}^p \in \Omega_{sc}^p$, Ω_{sc}^p is the signal set of x_{sc}^p with modulation order $K_f \times K_n$. (1) can be rewritten as:

$$x_{sc}^I + jx_{sc}^Q = \sqrt{\alpha_n}x_n^I + \sqrt{\alpha_f}x_f^I + j(\sqrt{\alpha_n}x_n^Q + \sqrt{\alpha_f}x_f^Q). \quad (3)$$

From (3) we have:

$$x_{sc}^p = \sqrt{\alpha_n}x_n^p + \sqrt{\alpha_f}x_f^p. \quad (4)$$

A. THE RELATIONSHIP BETWEEN CONSTELLATION PATTERN OF THE SC SIGNAL x_{sc}^p AND POWER ALLOCATION

There are $K_f \times K_n$ signal constellation points (SCP) in the signal set Ω_{sc}^p. Let Z_k^n, Z_l^f and Z_i^{sc} be the signal values of x_n^p, x_f^p and x_{sc}^p, where $k \in [1 : K_n]$, $l \in [1 : K_f]$ and $i \in [1 : K_f \times K_n]$. For convenience in discussion, we also let $Z_{k_1}^n < Z_{k_2}^n$ for $k_1 < k_2$ and $Z_{l_1}^f < Z_{l_2}^f$ for $l_1 < l_2$.

As an example, in this article we set $K_f = 2$, $K_n = 4$, $\alpha_f = 0.75$, $\alpha_n = 0.25$ and $E\{(x_n^p)^2\} = E\{(x_f^p)^2\} = 5$. We also set $Z_1^f = -\sqrt{5}$, $Z_2^f = +\sqrt{5}$, $Z_1^n = -3$, $Z_2^n = -1$, $Z_3^n = +1$ and $Z_4^n = +3$. Based on superposition coding of (4), the constellations of x_f^p, x_n^p and x_{sc}^p are shown in Figure 1.

The constellation pattern of the SC symbol depends on power allocation in the DL-NOMA system. This article will not discuss the power allocation in superposition coding. However, in order to make the DL-NOMA system work well, the power allocation in superposition coding of (4) must guarantee $Z_{1+lK_n}^{sc} > Z_{lK_n}^{sc}$. This is very important to signal detection.

As discussed in Section II, the guideline of the power allocation is $\alpha_f > \alpha_n$ and $\alpha_f + \alpha_n = 1$. Figure 1 shows the constellation of x_{sc}^p with $\alpha_f = 0.75$ and $\alpha_n = 0.25$, while Figure 2 shows the constellation of x_{sc}^p with $\alpha_f = 0.6$ and $\alpha_n = 0.4$. Both power allocation schemes meet $\alpha_f > \alpha_n$ and $\alpha_f + \alpha_n = 1$. In this example, from Figure 1 it is seen that $Z_5^{sc} > Z_4^{sc}$. Figure 1 also shows that $Z_{i_1}^{sc} < Z_{i_2}^{sc}$ for $i_1 < i_2$. However, the constellation pattern in Figure 2 shows that $Z_5^{sc} < Z_4^{sc}$, not $Z_5^{sc} > Z_4^{sc}$ which will not make the DL-NOMA system work well.

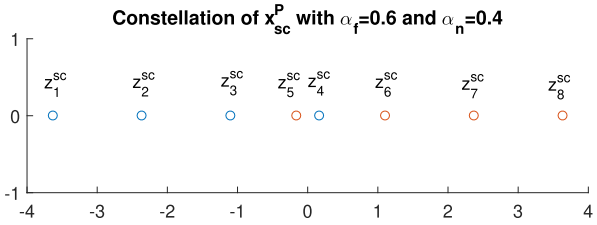

FIGURE 2. The constellation of x_{sc}^p with $\alpha_f = 0.6$ and $\alpha_n = 0.4$.

B. THE CONSTELLATION RELATIONSHIP BETWEEN SC SIGNAL x_{sc}^p AND FAR USER'S SIGNAL x_f^p

Based on superposition coding of (4), we can regard x_{sc}^p as a function of x_f^p and x_n^p, which is equivalent to Z_i^{sc} being a function of Z_k^f and Z_l^n. Let $f(\cdot, \cdot)$ be the function. Then we have:

$$Z_i^{sc} = f(Z_k^f, Z_l^n). \quad (5)$$

Now we discuss the constellation relationship between x_{sc}^p and x_f^p.

Given $x_f^p = Z_1^f$, it is observed from Figure 1 that $Z_1^{sc} = f(Z_1^f, Z_1^n)$, $Z_2^{sc} = f(Z_1^f, Z_2^n)$, $Z_3^{sc} = f(Z_1^f, Z_3^n)$ and $Z_4^{sc} = f(Z_1^f, Z_4^n)$. In general, we have $Z_{(k-1)K_n+l}^{sc} = f(Z_k^f, Z_l^n)$, where $l \in [1 : K_n]$ for the given k^{th} symbol of x_f^p, Z_k^f. The indexes of these K_n symbols $Z_{(k-1)K_n+l}^{sc}$ are consecutive, which is very important to the far user's signal detection and error performance analysis.

At the receiver, as long as User f detects that the transmitted x_{sc}^p is Z_i^{sc}, then based on the relationship $i = (k-1)K_n + l$, User f knows that the estimation of the transmitted x_f^p is Z_k^f. Again, as the example used in this article, if User f estimated that the transmitted x_{sc}^p is Z_k^{sc}, $k \in [1 : 4]$, then User f knows that the estimation of the transmitted x_f^p is Z_1^f.

C. THE CONSTELLATION RELATIONSHIP BETWEEN SC SIGNAL x_{sc}^p AND NEAR USER'S SIGNAL x_n^p

Given $x_n^p = Z_1^n$, it is observed from Figure 1 that $Z_1^{sc} = f(Z_1^f, Z_1^n)$ and $Z_5^{sc} = f(Z_2^f, Z_1^n)$. In general, we have $Z_{(k-1)K_n+l}^{sc} = f(Z_k^f, Z_l^n)$, where $k \in [1 : K_f]$ for the l^{th} symbol of x_n^p, Z_l^n. The indexes of these K_f symbols $Z_{(k-1)K_n+l}^{sc}$ are arithmetic numbers, which is also important to the near user's signal detection and error performance analysis.

At the receiver, as long as User n detects the transmitted x_{sc}^p is Z_i^{sc}, then based on the relationship $i = (k-1)K_n + l$, the User n knows the estimation of the transmitted x_n^p is Z_l^f. Again, as the example used in this article, if User n estimated that the transmitted x_{sc}^p is Z_1^{sc} or Z_5^{sc}, then User n knows that the estimation of the transmitted x_n^p is Z_1^n.

In this article, the above constellation relationships actually represent the equivalent models for the error performance analysis of the DL-NOMA system.

IV. SIGNAL DETECTIONS

In the DL-NOMA system, it is assumed that the channel state information (CSI) $\boldsymbol{h}_u$ is known at the receiver of User u. Based on the CSI, User n and User f detect their own symbol in different ways. In the following subsections, we discuss the signal detections for User n and User f, respectively. We firstly discuss the conventional detection for the far and near users, and then discuss the proposed threshold based detection for the far and near users.

A. CONVENTIONAL FAR USER SIGNAL DETECTION

The conventional far user signal detection has been described in [4] and [5]. The far user, User f, directly detects x_f by regarding the near user signal, x_n, as interference. By regarding x_n as interference, (2) may be rewritten as:

$$\boldsymbol{y}_f = \boldsymbol{h}_f\sqrt{\alpha_f}x_f + \bar{\boldsymbol{w}}_f, \tag{6}$$

where $\bar{\boldsymbol{w}}_f = \boldsymbol{h}_f\sqrt{\alpha_n}x_n + \boldsymbol{w}_f$.

Since $\boldsymbol{h}_f$ is known at the receiver of User f, we further have:

$$z_f = \frac{\boldsymbol{h}_f^H\boldsymbol{y}_f}{\|\boldsymbol{h}_f\|_F^2\sqrt{\alpha_f}} = x_f + v_f, \tag{7}$$

where $v_f = \frac{\boldsymbol{h}_f^H\bar{\boldsymbol{w}}_f}{\|\boldsymbol{h}_f\|_F^2\sqrt{\alpha_f}}$.

According to the maximum likelihood (ML) detection rule, the estimation of x_f at the receiver of User f is given by [5]:

$$\hat{x}_f = \min_{x_f\in\Omega_f} |z_f - x_f|^2. \tag{8}$$

B. SIC BASED NEAR USER SIGNAL DETECTION

At the receiver of User n, User n also needs to estimate the transmitted x_f. Similar to the above discussion in the previous subsection, the estimation of x_f at the receiver of User n can be obtained. Let the estimation of x_f at the receiver of User n be $\tilde{x}_f$. Then User n uses SIC to subtract $\tilde{x}_f$ from $\boldsymbol{y}_n$. Let $\hat{\boldsymbol{y}}_n = \boldsymbol{y}_n - \boldsymbol{h}_n\sqrt{\alpha_f}\tilde{x}_f$. $\hat{\boldsymbol{y}}_n$ can be written as:

$$\hat{\boldsymbol{y}}_n = \boldsymbol{h}_n\sqrt{\alpha_n}x_n + \hat{\boldsymbol{w}}_n, \tag{9}$$

where $\hat{\boldsymbol{w}}_n = \boldsymbol{h}_n\sqrt{\alpha_f}(x_f - \tilde{x}_f) + \boldsymbol{w}_n$.

Again, since $\boldsymbol{h}_n$ is known at the receiver of User n, we further have:

$$z_n = \frac{\boldsymbol{h}_n^H\hat{\boldsymbol{y}}_n}{\|\boldsymbol{h}_n\|_F^2\sqrt{\alpha_n}} = x_n + v_n, \tag{10}$$

where $v_n = \frac{\boldsymbol{h}_n^H\hat{\boldsymbol{w}}_n}{\|\boldsymbol{h}_n\|_F^2\sqrt{\alpha_n}}$.

Based on the ML detection, the estimation of x_n is finally given by:

$$\hat{x}_n = \min_{x_n\in\Omega_n} |z_n - x_n|^2. \tag{11}$$

From the above signal detection for both the far user and near user, the following is evident:

1) Equs. (8) and (11) represent the ML detection. The detection complexity of (8) and (11) can be reduced by detecting the in-phase and quadrature components of x_f and x_n, respectively.
2) In (6), $\bar{\boldsymbol{w}}_f = \boldsymbol{h}_f\sqrt{\alpha_n}x_n + \boldsymbol{w}_f$. The distribution of x_n is uniform, while the distribution of each entry in $\boldsymbol{w}_f$ is Gaussian distributed. It is not easy to derive the PDF for the entry of $\bar{\boldsymbol{w}}_f$, and to further analyze the error performance of x_f.

Motivated by the above observation and the constellation relationship between x_{sc}^p and x_u^f, in the following subsections, we present a simple and low complexity detection algorithm, threshold based signal detection, to detect the in-phase and quadrature components of x_f and x_n.

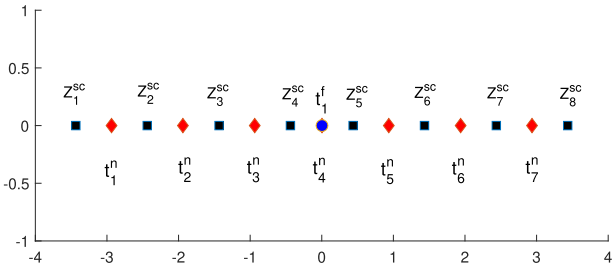

FIGURE 3. The constellations of x_{sc}^p and thresholds t_k^f and t_l^n.

C. THRESHOLD BASED FAR USER'S SIGNAL DETECTION

Since both the received signal $\boldsymbol{y}_f$ and $\boldsymbol{h}_f$ in (2), are known at the receiver of User f, we have:

$$z_f = \frac{\boldsymbol{h}_f^H\boldsymbol{y}_f}{\|\boldsymbol{h}_f\|_F^2} = x_{sc} + v_f, \tag{12}$$

where $v_f = \frac{\boldsymbol{h}_f^H\boldsymbol{w}_f}{\|\boldsymbol{h}_f\|_F^2}$.

Following (4), we rewrite (12) as:

$$z_f^p = x_{sc}^p + v_f^p. \tag{13}$$

As discussed in Section III, there are K_n possible symbols of x_{sc}^p, $Z_{(k-1)K_n+l}^{sc}$ for a given k^{th} symbol of x_f^p, Z_k^f. When one of $x_{sc}^p = Z_i^{sc}$ is transmitted, $i \in [1+(k-1)K_n : kK_n]$ the estimation of x_f^p should be Z_k^f for $t_{k-1}^f < z_f^p < t_k^f$, where both t_{k-1}^f and t_k^f are thresholds which are used to detect Z_k^f. Since there are K_f symbols of x_f^p, we need to find $K_f - 1$ thresholds for detecting x_f^p. These $K_f - 1$ thresholds t_k^f, $k \in [1 : K_f - 1]$ are easily derived as:

$$t_k^f = Z_{kK_n}^{sc} + \frac{Z_{kK_n+1}^{sc} - Z_{kK_n}^{sc}}{2}. \tag{14}$$

For convenience in discussion in the next subsection, we set $t_0^f = -\infty$ and $t_{K_f}^f = \infty$ in (14). For the above example, only one threshold, t_1^f is also shown in Figure 3.

Generally, based on z_f^p in (13), and the threshold t_k^f in (14), the estimation of x_f^p can be easily implemented based on Algorithm 1:

D. THRESHOLD BASED NEAR USER'S SIGNAL DETECTION

Similar to the discussion in the previous subsection, the received signal at the receiver of User n is given by:

$$z_n^p = x_{sc}^p + v_n^p. \tag{15}$$

Algorithm 1 Threshold Based Signal Detection for Far User

Input: A list of thresholds $[t_i^f]$, $i = [1 : K_f - 1]$, a list of standard outputs Z_k^f, $k = [1 : K_f]$ and z_f^p.
Output: $\hat{x}_f^p$
$\hat{x}_f^p \leftarrow Z_1^f$;
for $i \leftarrow 1$ **to** $K_f - 1$ **do**
  if $z_f^p > t_i^f$ **then**
    $\hat{x}_f^p \leftarrow Z_{i+1}^f$;
  end if
end for

Algorithm 2 Threshold Based Signal Detection for Near User: Step 1

Input: A list of thresholds $[t_l^f]$, $l = [0 : K_f]$ and z_n^p.
Output: $t_l^f < z_n^p < t_{l+1}^f$
$t_0^f < z_n^p < t_1^f$;
for $l \leftarrow 1$ **to** $K_f - 1$ **do**
  if $z_n^p > t_l^f$ **then**
    $t_l^f < z_n^p < t_{l+1}^f$;
  end if
end for

Based on Algorithm 1, it is easy to find that $z_n^p > t_k^f$. From the constellation relationship between x_{sc}^p and x_f^p discussed in Section III, it is known that the estimation of the transmitted symbol x_n^p is in the range between t_k^f and t_{k+1}^f. There are K_n symbols of x_{sc}^p between t_k^f and t_{k+1}^f. Now we apply Algorithm 1 again to estimate the transmitted x_n^p in the range between t_k^f and t_{k+1}^f. We need $K_n - 1$ thresholds to detect x_n^p in each range between t_k^f and t_{k+1}^f in Algorithm 1. These $K_n - 1$ thresholds between t_k^f and t_{k+1}^f can also be easily calculated as:

$$t_{kK_n+l}^n = Z_{kK_n+l}^{sc} + \frac{Z_{kK_n+l+1}^{sc} - Z_{kK_n+l}^{sc}}{2}. \tag{16}$$

These thresholds $t_k^n, k \in [1 : K_f \times K_n - 1]$ are shown in Figure 3. Based on the proposed threshold based detection algorithm, the estimation of x_n^p takes two steps.

Step 1: Apply the proposed threshold based detection algorithm in the previous subsection to find $t_l^f < z_n^p < t_{l+1}^f$, $l \in [0 : K_f - 1]$, which is shown in Algorithm 2.

Step 2: Between t_l^f and t_{l+1}^f, apply the proposed threshold based detection algorithm to find the estimation of $x_n^p, \hat{x}_n^p$.

From Figure 3, it is found that the thresholds for detecting x_n^p are $t_i^n, i \in [lK_n + 1 : (l+1)K_n - 1]$ between t_l^f and t_{l+1}^f. Applying the proposed threshold detection algorithm to find the estimation of x_n^p is shown in Algorithm 3.

Algorithm 3 Threshold Based Signal Detection for Near User: Step 2

Input: A list of thresholds $[t_{lK_n+k}^n]$, $k = [1 : K_n - 1]$, a list of standard outputs Z_k^n, $k = [1 : K_n]$ and z_n^p.
Output: $\hat{x}_n^p$
$\hat{x}_n^p \leftarrow Z_1^n$;
for $k \leftarrow 1$ **to** $K_n - 1$ **do**
  if $z_n^p > t_{lK_n+k}^n$ **then**
    $\hat{x}_n^p \leftarrow Z_{k+1}^n$;
  end if
end for

E. COMPLEXITY ANALYSIS OF THE THRESHOLD BASED SIGNAL DETECTION

Compared to the detection in (8), the proposed Algorithm 1 will not treat x_n as an interference to detect the far user's signal. The proposed Algorithm 1 only requires comparison, and not the norm operation. Hence, the detection complexity of Algorithm 1 is less than (8).

Compared to the SIC based detection of x_n in (11), the proposed Algorithm 2 and 3 do not use SIC and/or norm operations to detect the near user's signal. The proposed Algorithm 2 and 3 also only need comparisons. Hence, once again the detection complexity of Algorithms 2 and 3 is much lower than (11).

In the following discussion, we regard that the complexity of the conventional detection and the proposed threshold based detection is in terms of real operations. It is also assumed that one complex operation is equal to four real operations averagely [14].

In (7), $\boldsymbol{h}_f^H \boldsymbol{y}_f$ takes N_r complex multiplications and $N_r - 1$ complex additions, which is equal to $4(2N_r - 1)$ real operations. It is easy to calculate that $\|\boldsymbol{h}_f\|_F^2 \sqrt{\alpha_f}$ in (7) takes $4N_r$ real operations. Finally, the division $\frac{\boldsymbol{h}_f^H \boldsymbol{y}_f}{\|\boldsymbol{h}_f\|_F^2 \sqrt{\alpha_f}}$ in (7), needs two real operations. Totally from $\boldsymbol{y}_f$ to (7), it takes $12N_r - 2$ real operations.

For the far user's signal detection, (7) also can be rewritten as:

$$z_f^p = x_f^p + v_f^p, \tag{17}$$

where $p \in [I, Q]$. Based on the ML detection, the estimation of x_f^p is given by:

$$\hat{x}_f^p = \min_{x_f^p \in \Omega_f^p} |z_f^p - x_f^p|^2. \tag{18}$$

In (18), given a $x_f^p \in \Omega_f^p$ $|z_f^p - x_f^p|^2$ costs two real operations. If we use the sort$(\cdot)$ function to implement the function min$(\cdot)$ in (18), the complexity is $K_f \log_2 K_f$ real operations [15]. (18) needs $2K_f + K_f \log_2 K_f$ real operations for in-phase or quadrature signal detection. For the conventional detector to detect one complex far user signal, the overall number of real operations is given by:

$$\delta_c^f = 12N_r + 4K_f + 2K_f \log_2 K_f - 2 \tag{19}$$

However, for the proposed threshold based detector to detect one complex far user signal, the overall number of real operations is given by:

$$\delta_p^f = 12N_r + 2K_f - 4 \tag{20}$$

In the conventional detection, User n detects the far user's signal first, and then detects its signal based on SIC. From the above discussion, the near user needs δ_c^f real operations to detect the far user's signal. In (9), $\boldsymbol{y}_n - \boldsymbol{h}_n\sqrt{\alpha_f}\tilde{x}_f$ costs N_r complex multiplications and N_r subtractions, which is equal to $8N_r$ real operations. Similar to the above discussion, from $\boldsymbol{y}_n$ to (10), it takes $12N_r - 2$ real operations. For the near user's signal detection, (11) also can be rewritten as:

$$z_n^p = x_n^p + v_n^p. \tag{21}$$

Based on the ML detection, the estimation of x_n^p is given by:

$$\hat{x}_n^p = \min_{x_n^p \in \Omega_n^p} |z_n^p - x_n^p|^2. \tag{22}$$

(22) needs $2K_n + K_n\log_2 K_n$ real operations for in-phase or quadrature signal detection. For SIC based detector to detect one complex near user signal, the overall number of real operations is given by:

$$\delta_c^n = \delta_c^f + 20N_r + 4K_n + 2K_n\log_2 K_n - 2. \tag{23}$$

For the proposed threshold based detection, Algorithm 2 needs $K_f - 1$ real operations, and Algorithm 3 needs $K_n - 1$ real operations. For the proposed threshold based detector to detect one complex near user signal, the overall number of real operations is given by:

$$\delta_p^n = 12N_r + 2K_f + 2K_n - 6. \tag{24}$$

Define the percentage of complexity reduction for the proposed threshold based detection compared to the conventional detection as:

$$\beta^u = \frac{\delta_c^u - \delta_p^u}{\delta_c^u} \times 100, \tag{25}$$

where $u \in [f, n]$. β^f and β^n are the percentage of complexity reduction for the far user and near user, respectively.

Again, as an example, we set $K_f = 2$ and $K_n = 4$. The proposed threshold based detection results $\beta^f = 45.45\%$ and $\beta^n = 75\%$ complexity reduction for $N_r = 1$, and $\beta^f = 29.41\%$ and $\beta^n = 71.15\%$ complexity reduction for $N_r = 2$, respectively.

From the above complexity analysis and discussion, it is easy to find that the proposed threshold based detection has low detection complexity compared to the SIC based conventional detection.

V. ASEP ANALYSIS OF THE DL-NOMA SYSTEM

Based on the literature survey for the error performance analysis in Section I, most of the work derived error performance based on SIC. Only [5] derived error performance in Gaussian channel by considering the relationship between PAM and QAM. In this article, we did not derive error performance for the individual user directly. We convert the derivation of error performance for the individual user's symbol into the error performance of the SC symbols based on the constellation relationship between x_{sc}^p and x_u^p. This approach is straightforward and easy to understand.

In this article, the error performance analysis for the DL-NOMA system is directly based on the transmission of x_{sc} over the AWGN channel. The received signal is given by:

$$r_{sc} = x_{sc} + n_{sc}, \tag{26}$$

where n_{sc} is a complex Gaussian RV distributed as $CN(0, \frac{\varepsilon}{\rho})$.

Following (4), (26) is further written as:

$$r_{sc}^p = x_{sc}^p + n_{sc}^p, \tag{27}$$

where n_{sc}^p is a Gaussian RV distributed as $N(0, \frac{\varepsilon}{2\rho})$.

Let $p_u(e)$ be the average error probability of either the in-phase or quadrature component of x_u, and $p_u^s(e)$ be the symbol error probability (SEP) of x_u, $u \in [f, n]$. Since QAM is composed of independent and identical in-phase and quadrature components, the SEP $p_u^s(e)$ may be expressed as:

$$p_u^s(e) = 2p_u(e) - (p_u(e))^2. \tag{28}$$

Since there are K_u signal values of x_u^p, $p_u(e)$ may be expressed as:

$$p_u(e) = \sum_{k=1}^{K_u} p(e|x_u^p = Z_k^u)p(x_u^p = Z_k^u), \tag{29}$$

where $p(e|x_u^p = Z_k^u)$ is the error probability when $x_u^p = Z_k^u$ is transmitted.

If $x_u^p = Z_k^u$ were directly transmitted, $p(e|x_u^p = Z_k^u)$ would be easily derived. However the DL-NOMA system transmits x_{sc}^p, not x_u^p. At the receiver of User u only $x_{sc}^p + v_{sc}^p$ is known, and $x_u^p + v_u^p$ is not known. Thus, we need to derive the error performance of the DL-NOMA system based on the received $x_{sc}^p + v_{sc}^p$. As discussed in Section III, there exist two constellation relationships between x_{sc}^p and x_f^p, and between x_{sc}^p and x_n^p. Now we derive the ASEP for the far user and near user, respectively.

A. ASEP OF FAR USER OVER AWGN

Based on superposition coding, transmitting $x_f^p = Z_k^f$ is equivalent to transmitting one of K_n SC symbols $x_{sc}^p = Z_i^{sc}$, $i \in [1 + (k-1)K_n : kK_n]$, where $k \in [1 : K_f]$. As an example, in this article, we set $K_f = 2$ and $K_n = 4$. Suppose Z_1^f is transmitted. Then transmitting Z_1^f is equivalent to the transmission of one of four symbols: $Z_1^{sc}, Z_2^{sc}, Z_3^{sc}$ or Z_4^{sc}. This is shown in Figure 3. From Figure 3 it is observed that if any one of the above four symbols Z_i^{sc}, $i \in [1 : 4]$ is transmitted, an unsuccessful detection of $x_f^p = Z_1^f$ occurs when the received signal of (27) satisfies the condition $r_{sc}^p > t_1^f$.

In general, there are $K_n \times K_f$ SC symbols $x_{sc}^p = Z_i^{sc}$, $i \in [1 : K_n \times K_f]$. There are $K_f - 1$ thresholds t_k^f, $k \in [1 : K_f - 1]$ to detect x_f^p. As discussed before we also have $t_0^f = -\infty$ and $t_{K_f}^f = \infty$.

Define $p(e|x_f^p = Z_k^f)$ as the error probability when $x_f^p = Z_k^f$ is transmitted. Similar to the above discussion and analysis, the derivation of $p(e|x_f^p = Z_f^k)$ is equivalent to finding $p(e_f|x_{sc}^p = Z_k^{sc})$, which is defined as the error probability of detecting x_f^p when $x_{sc}^p = Z_k^{sc}$ is transmitted. Thus, in terms of transmission of x_{sc}^p, the ASEP for the far user $p_f(e)$ is alternatively given by:

$$p_f(e) = \sum_{k=1}^{K_n \times K_f} p(e_f|x_{sc}^p = Z_k^{sc}) p(s_{sc}^p = Z_k^{sc}), \tag{30}$$

where $p(s_{sc}^p = Z_k^{sc}) = \frac{1}{K_n \times K_f}$.

From Figure 3, it is seen that $p(e_f|x_{sc}^p = Z_k^{sc})$ in (30), is given by:

$$\begin{aligned} &p(e_f|x_{sc}^p = Z_k^{sc}) \\ &\quad = p(Z_k^{sc} + n_{sc}^p < t_a^f) \bigcup p(Z_k^{sc} + n_{sc}^p > t_{a+1}^f), \end{aligned} \tag{31}$$

where $a = \lfloor \frac{k}{K_n + \delta} \rfloor$, $\lfloor x \rfloor$ is the floor function and δ is a very small positive rational number.

Since $t_0^f = -\infty$ and $t_{K_f}^f = +\infty$. Then $p(Z_k^{sc} + n_{sc}^p < t_0^f) = 0$ and $p(Z_k^{sc} + n_{sc}^p > t_{K_f}^f) = 0$ in (31).

According to $t_{a+1}^f > Z_{sc}^k$ and $Z_{sc}^k > t_a^f$, (31) can be further written as:

$$p(e|x_{sc}^p = Z_k^{sc}) = p(n_{sc}^p > Z_k^{sc} - t_a) \bigcup p(n_{sc}^p > t_{a+1} - Z_k^{sc}). \tag{32}$$

We further have that:

$$p(e|x_{sc}^p = Z_k^{sc}) = Q\left(\sqrt{d_{2k-1}^f \rho}\right) + Q\left(\sqrt{d_{2k}^f \rho}\right), \tag{33}$$

where $Q(\cdot)$ is the Gaussian Q-function, $d_{2k-1}^f = \frac{2(Z_k^{sc} - t_a)^2}{\varepsilon}$ and $d_{2k}^f = \frac{2(t_{a+1} - Z_k^{sc})^2}{\varepsilon}$.

Finally, the error probability $p_f(e)$ over the AWGN channel is given by:

$$p_f(e) = A \sum_{l=1}^{2K} Q\left(\sqrt{d_l^f \rho}\right), \tag{34}$$

where $K = K_n \times K_f$ and $A = \frac{1}{K}$.

B. ASEP OF NEAR USER OVER AWGN

Based on superposition coding, transmitting $x_n^p = Z_k^n$ is equivalent to transmitting one of K_f SC symbols $x_{sc}^p = Z_i^{sc}$, $i \in [(l-1) \times K_n + k]$, where $l \in [1 : K_f]$. Again, we set $K_f = 2$ and $K_n = 4$ as an example in Figure 3. Suppose Z_1^n is transmitted. Transmitting Z_1^n is equivalent to the transmission of one of two symbols: Z_1^{sc} and Z_5^{sc}.

From Figure 3, it is seen that if Z_1^{sc} is transmitted, a successful detection of $x_n^p = Z_1^n$ occurs when the received signal of (27) satisfies the condition $-\infty < r_{sc}^p < t_1^n$ or $t_4^n < r_{sc}^p < t_5^n$. Similarly, from Figure 3 it is also seen that if Z_5^{sc} is transmitted, a successful detection of $x_n^p = Z_1^n$ occurs when the received signal of (27) also satisfies the condition $-\infty < r_{sc}^p < t_1^n$ or $t_4^n < r_{sc}^p < t_5^n$. Actually if Z_1^{sc} is transmitted, the probability of $-\infty < r_{sc}^p < t_1^n$ is much larger than the one of $t_4^n < r_{sc}^p < t_5^n$. Similarly, if Z_5^{sc} is transmitted, the probability of $t_4^n < r_{sc}^p < t_5^n$ is much larger than one of $-\infty < r_{sc}^p < t_1^n$. Thus, in the following discussion, we only take into account $t_{k-1}^n < r_{sc}^p < t_k^n$ when Z_k^{sc} is transmitted. For convenience, we also let $t_0^n = -\infty$ and $t_{K_f \times K_n}^n = +\infty$.

Similar to the above discussion in the previous subsection, $p_n(e)$ is alternatively given by:

$$p_n(e) = 1 - \sum_{k=1}^{K_n \times K_f} p(c_n|x_{sc}^p = Z_k^{sc}) p(x_{sc}^p = Z_k^{sc}), \tag{35}$$

where $p(x_{sc}^p = Z_k^{sc})$ is given in (30) and $p(c_n|x_{sc}^p = Z_k^{sc})$ is defined as the correct probability of detecting x_n^p when $x_{sc}^p = Z_k^{sc}$ is transmitted.

From Figure 3, it is seen that $p(c_n|x_{sc}^p = Z_k^{sc})$ in (35) is given by:

$$p(c_n|x_{sc}^p = Z_k^{sc}) = p(t_{k-1}^n < Z_k^{sc} + n_{sc}^p < t_k^n). \tag{36}$$

We further have that:

$$p(c_n|x_{sc}^p = Z_k^{sc}) = 1 - \left(Q\left(\sqrt{d_{2k-1}^n \rho}\right) + Q\left(\sqrt{d_{2k}^n \rho}\right)\right), \tag{37}$$

where $d_{2k-1}^n = \frac{2(Z_k^{sc} - t_{k-1}^n)^2}{\varepsilon}$ and $d_{2k}^n = \frac{2(t_k^n - Z_k^{sc})^2}{\varepsilon}$.

Finally, the error probability $p_n(e)$ over the AWGN channel is given by:

$$p_n(e) = A \sum_{l=1}^{2K} Q\left(\sqrt{d_l^n \rho}\right). \tag{38}$$

C. ASEPs OF FAR AND NEAR USERS IN RAYLEIGH FADING CHANNELS

The SEP of both User f and User n over AWGN has been shown in (28). In this subsection, we will derive the symbol error probability of both User f and User n in Rayleigh fading channels based on the received signal in (2).

Given $\boldsymbol{h}_u$, $p_u^s(e)$ in (28) becomes $p_u^s(e|\boldsymbol{h}_u)$. ρ in (34) and (38) becomes $\|\boldsymbol{h}_f\|_F^2 \rho$ and $\|\boldsymbol{h}_n\|_F^2 \rho$, respectively. Define the instantaneous SNR at the receiver of User u as $\gamma_u = \frac{P_s}{P_n} = \|\boldsymbol{h}_u\|_F^2 \rho$, where P_s is the instantaneous signal power and P_n is the instantaneous noise power. The PDF of γ_u is given by [16]:

$$f_{\gamma_u}(\gamma_u) = \frac{1}{(N_r - 1)! \bar{\gamma}_u^{N_r}} \gamma_u^{N_r - 1} e^{-\frac{\gamma_u}{\bar{\gamma}_u}}, \tag{39}$$

where $\bar{\gamma}_u = \sigma_u^2 \rho$.

Finally, the ASEP of User u in the Rayleigh fading channel is given by:

$$p_u^s(e) = \int_0^{+\infty} p_u^s(e|\boldsymbol{h}_u) f_{\gamma_u}(\gamma_u) d\gamma_u, \tag{40}$$

where $p_u^s(e|\boldsymbol{h}_u) = 2p_u(e|\boldsymbol{h}_u) - p_u^2(e|\boldsymbol{h}_u)$.

In order to derive closed-form ASEP expressions, we need to approximate the Gaussian Q-function in (40) for integration. Taking into account conciseness of ASEP expressions and approximation accuracy we approximate the Q-function in $2p_u(e|\boldsymbol{h}_u)$ using the trapezoidal rule, while we approximate

TABLE 1. Parameters setting for simulation.

M_f	M_n	α_f	α_n	σ_f^2	σ_n^2
4	16	0.7619	0.2381	0.5	1
16	16	0.95	0.05	0.5	1

the Q-function in $p_u^2(e|\boldsymbol{h}_u)$ using the exponential bound in [17]. The Gaussian Q-function based on the trapezoidal rule may be approximated as:

$$Q(x) \approx \frac{1}{2c}\Big[\frac{1}{2}e^{-\frac{x^2}{2}} + \sum_{k=1}^{c-1} e^{-\frac{x^2}{2s_k}}\Big], \tag{41}$$

where $s_k = \sin^2(k\pi/(2c))$ and c is the number of partitions for the integration in the Q-function.

The Gaussian Q-function using the exponential bound may be approximated as:

$$Q(x) \approx \frac{1}{12}e^{-\frac{x^2}{2}} + \frac{1}{4}e^{-\frac{2x^2}{3}}. \tag{42}$$

Substituting (39), (41) and (42) into (40), the ASEP $p_u^s(e)$ for User u in the Rayleigh fading channel may be derived as:

$$p_u^s(e) = 2A\sum_{l=1}^{2K} m_G(d_l^u) + A^2\sum_{k=1}^{2K}\sum_{l=1}^{2K} m_P(d_k^u, d_l^u), \tag{43}$$

where $m_G(x)$ is defined as:

$$\begin{aligned} m_G(x) &= \int_0^{+\infty} Q\left(\sqrt{x\gamma_u}\right) f_{\gamma_u}(\gamma_u) d\gamma_u, \\ &= \frac{1}{4c}\Big((1+0.5x\bar{\gamma}_u)^{-N_r} + 2\sum_{k=1}^{c-1}(1+0.5x\bar{\gamma}_u s_k^{-1})^{-N_r}\Big), \end{aligned} \tag{44}$$

and $m_P(x_1, x_2)$ is defined as:

$$\begin{aligned} m_P(x_1, x_2) &= \int_0^{+\infty} Q\left(\sqrt{x_1\gamma_u}\right) Q\left(\sqrt{x_2\gamma_u}\right) f_{\gamma_u}(\gamma_u) d\gamma_u, \\ &= \sum_{k=1}^{4}(1 + a_k\bar{\gamma}_u)^{-N_r}, \end{aligned} \tag{45}$$

with $a_1 = \frac{x_1+x_2}{2}$, $a_2 = \frac{3x_1+4x_2}{6}$, $a_3 = \frac{4x_1+3x_2}{6}$ and $a_4 = \frac{2x_1+2x_2}{3}$.

VI. NUMERICAL RESULTS

In this section, we present the simulated symbol error rate (SER) versus SNR results for the DL-NOMA system. In the simulation, it is assumed that the channel fading coefficients $\boldsymbol{h}_f$ and $\boldsymbol{h}_n$ with AWGN are the same as discussed in Section II. Both $N_r = 1$ and $N_r = 2$ are considered in this article. The remaining simulation parameters are tabulated in Table 1.

It is further assumed that the CSI is fully known at the receiver of User f and User n. We also calculate the theoretical results of (43) and validate these theoretical results by simulations.

Figures 4 and 5 demonstrate the SER versus SNR results of the DL-NOMA system with $M_f = 4, M_n = 16$ and $M_f = 16, M_n = 16$, respectively. The theoretical ASEPs of (43) are also plotted in Figures 4 and 5. In the legend,

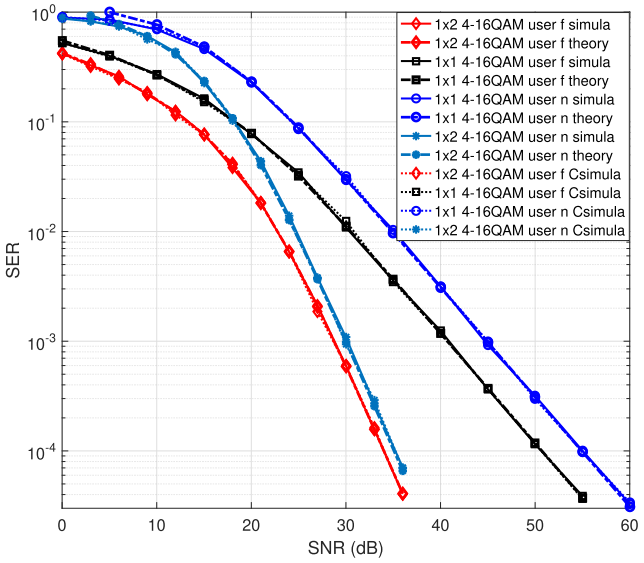

FIGURE 4. SER versus SNR performance of the far user and near user in the DL-NOMA system with 4-16QAM.

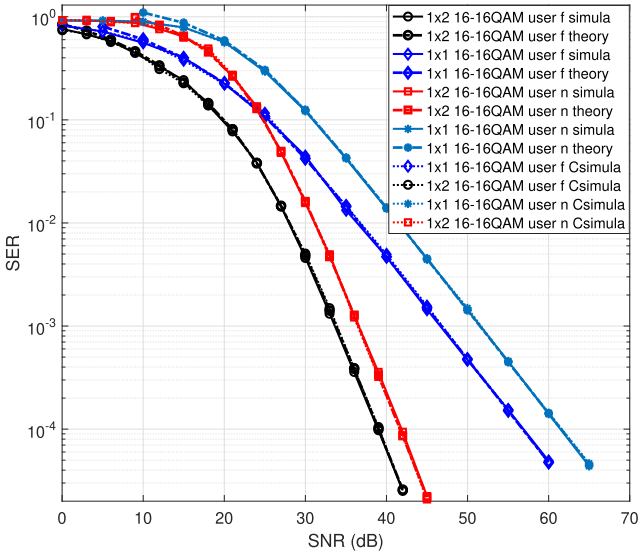

FIGURE 5. SER versus SNR performance of the far user and near user in the DL-NOMA system with 16-16QAM.

"$1 \times N_r$ M_f-M_nQAM User u Csimula, simula or theory", $1 \times N_r$ denotes that the BS is equipped with one transmit antenna, and User u is equipped with N_r receiver antennas; M_f-M_nQAM denotes that the symbols to be transmitted to User f and User n are M_fQAM and M_nQAM, respectively; "Csimula, simula or theory" denote simulation based on conventional detection, simulation based on proposed threshold based detection and theoretical results based on (43), respectively.

From Figures 4 and 5, it is observed that the symbol error performance of the proposed threshold based detection is identical to the one of the conventional detection. It is also observed that the theoretical results are worse than simulation results at very low SNR. This is caused by the low accuracy of the approximated Q-function using the exponential bound.

However, it is also observed that the theoretical results match very well with the simulation results for other SNR ranges for two DL-NOMA systems with $N_r = 1$ and $N_r = 2$.

VII. CONCLUSION

In this article, we investigated the signal constellation relationship between the individual user's signal and the SC signal. Based on the constellation relationships, we proposed a simple signal detection scheme, threshold based detection for both far and near users. Compared to the conventional detection, the proposed threshold detection does not treat the near user's signal as interference at the receiver of the far user, and also does not use SIC to detect its signal at the receiver of the near user. The detection complexity for both the conventional detection and the proposed threshold based detection was analyzed. We further derived closed-form ASEP expressions for both the far user and near user based on the constellation relationships. Finally, we presented the simulation results which served to validate the theoretical frameworks. In future, we will directly extend the proposed threshold based detection algorithm and the derivation of the ASEP into multi-user DL-NOMA system with multiple receive antennas. We may also extend the work of this article into other channel fading models.

REFERENCES

[1] V. W. S. Wong, R. Schober, D. W. K. Ng, and L. Wang, *Key Technologies for 5G Wireless Systems*. Cambridge, U.K.: Cambridge Univ. Press, 2017.

[2] L. Dai, B. Wang, Y. Yuan, S. Han, C.-L. I, and Z. Wang, "Non-orthogonal multiple access for 5G: Solutions, challenges, opportunities, and future research trends," *IEEE Commun. Mag.*, vol. 53, no. 9, pp. 74–81, Sep. 2015.

[3] W. Shin, M. Vaezi, B. Lee, D. J. Love, J. Lee, and H. V. Poor, "Non-orthogonal multiple access in multi-cell networks: Theory, performance, and practical challenges," *IEEE Commun. Mag.*, vol. 55, no. 10, pp. 176–183, Oct. 2017.

[4] F. Kara and H. Kaya, "BER performances of downlink and uplink NOMA in the presence of SIC errors over fading channels," *IET Commun.*, vol. 12, no. 15, pp. 1834–1844, Sep. 2018.

[5] Q. He, Y. Hu, and A. Schmeink, "Closed-form symbol error rate expressions for non-orthogonal multiple access systems," *IEEE Trans. Veh. Technol.*, vol. 68, no. 7, pp. 6775–6789, Jul. 2019.

[6] L. Bariah, S. Muhaidat, and A. Al-Dweik, "Error probability analysis of non-orthogonal multiple access over Nakagami-*m* fading channels," *IEEE Trans. Commun.*, vol. 67, no. 2, pp. 1586–1599, Feb. 2019.

[7] T. Assaf, A. Al-Dweik, M. E. Moursi, and H. Zeineldin, "Exact BER performance analysis for downlink NOMA systems over Nakagami-*m* fading channels," *IEEE Access*, vol. 7, pp. 134539–134555, 2019.

[8] I.-H. Lee and J.-B. Kim, "Average symbol error rate analysis for non-orthogonal multiple access with *M* -Ary QAM signals in Rayleigh fading channels," *IEEE Commun. Lett.*, vol. 23, no. 8, pp. 1328–1331, Aug. 2019.

[9] Y. Zhang, J. Ge, and E. Serpedin, "Performance analysis of nonorthogonal multiple access for downlink networks with antenna selection over Nakagami-m fading channels," *IEEE Trans. Veh. Technol.*, vol. 66, no. 11, pp. 10590–10594, Nov. 2017.

[10] J. Men, J. Ge, and C. Zhang, "Performance analysis for downlink relaying aided non-orthogonal multiple access networks with imperfect CSI over Nakagami-*m* fading," *IEEE Access*, vol. 5, pp. 998–1004, 2017.

[11] Z. Ding, R. Schober, and H. V. Poor, "A general MIMO framework for NOMA downlink and uplink transmission based on signal alignment," *IEEE Trans. Wireless Commun.*, vol. 15, no. 6, pp. 4438–4454, Jun. 2016.

[12] J.-B. Kim and I.-H. Lee, "Capacity analysis of cooperative relaying systems using non-orthogonal multiple access," *IEEE Commun. Lett.*, vol. 19, no. 11, pp. 1949–1952, Nov. 2015.

[13] Z. Wei, L. Yang, D. W. K. Ng, J. Yuan, and L. Hanzo, "On the performance gain of NOMA over OMA in uplink communication systems," *IEEE Trans. Commun.*, vol. 68, no. 1, pp. 536–568, Jan. 2020.

[14] H. Xu and N. Pillay, "The component-interleaved golden code and its low-complexity detection," *IEEE Access*, vol. 8, pp. 65649–65657, 2020.

[15] T. H. Cormen, C. E. Leiserson, R. L. Rivest, and C. Stein, *Introduction to Algorithms*, 3rd ed. Cambridge, MA, USA: MIT Press, 2009.

[16] M. K. Simon and M.-S. Alouini, *Digital Communication Over Fading Channels: A Unified Approach to Performance Analysis*. Hoboken, NJ, USA: Wiley-Interscience Publication, 2000.

[17] M. Chiani, D. Dardari, and M. K. Simon, "New exponential bounds and approximations for the computation of error probability in fading channels," *IEEE Trans. Wireless Commun.*, vol. 24, no. 5, pp. 840–845, May 2003.

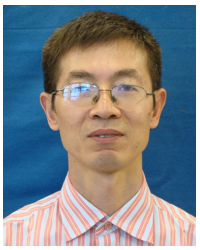

HONGJUN XU (Member, IEEE) received the B.Sc. degree from the Guilin University of Electronic Technology, China, in 1984, the M.Sc. degree from the Institute of Telecontrol and Telemeasure, Shijianzhuang, China, in 1989, and the Ph.D. degree from the Beijing University of Aeronautics and Astronautics, Beijing, China, in 1995. He also did postdoctoral research at the University of Natal and Inha University, from 1997 to 2000. He is currently a Full Professor with the School of Engineering, University of KwaZulu-Natal, Howard College Campus. He is also a National Research Foundation (NRF) Rated Researcher in South Africa. He has published more than 50 journal articles. His research interests include digital and wireless communications and digital systems.

NARUSHAN PILLAY received the M.Sc.Eng. *(cum laude)* and Ph.D. degrees in wireless communications from the University of KwaZulu-Natal, Durban, South Africa, in 2008 and 2012, respectively. He has been with the University of KwaZulu-Natal, since 2009. Previously, he was with the Council of Scientific and Industrial Research (CSIR), South Africa. He currently supervises several Ph.D. and M.Sc.Eng. students. His research interest includes physical wireless communications, including spectrum sensing for cognitive radio and MIMO systems. He has published several articles in well-known journals in his area of research.